

Zee models with a non-invertible Z_M symmetry

Huiji Jin,^{1,*} Takaaki Nomura,^{1,†} and Hiroshi Okada^{2,‡}

¹*College of Physics, Sichuan University, Chengdu 610065, China*

²*Department of Physics, Henan Normal University, Xinxiang 453007, China*

(Dated: May 25, 2026)

Abstract

We investigate Zee models by incorporating a non-invertible Z_M symmetry. The models are systematically classified based on their symmetry assignments, which dictate structures for the Yukawa couplings and the neutrino mass matrix. By evaluating the consistency of these mass structures with current experimental data, we identify the viable model candidates. Focusing on a representative benchmark model based on the non-invertible Z_7 symmetry, we perform a detailed numerical analysis. Our results yield characteristic predictions for neutrino observables and charged lepton flavor violating processes within the allowed parameter space.

arXiv:2605.23202v1 [hep-ph] 22 May 2026

*Electronic address: jinhuiji@stu.scu.edu.cn

†Electronic address: nomura@scu.edu.cn

‡Electronic address: hiroshi3okada@htu.edu.cn

I. INTRODUCTION

The origin of neutrino masses and mixings remains one of the compelling questions in particle physics, pointing directly toward the physics beyond the standard model (BSM). In fact, numerous BSM frameworks have been proposed to generate neutrino masses, ranging from tree-level mechanisms to various loop-level contributions [1]. Within these frameworks, a key challenge is to achieve a predictive structure of neutrino mass matrix which naturally accommodates the observed neutrino oscillation data.

Among the various radiative mechanisms, the Zee model stands out as a highly attractive candidate, where the neutrino masses are induced at the one-loop level [2]. By extending the scalar sector with a second Higgs doublet and a charged scalar field, the model provides a rich phenomenological landscape. While the general Zee model can fit current neutrino data, its predictability is often limited by the large number of free parameters in the Yukawa sector [3]. To enhance predictability, various symmetries have been adopted; for instance, the original Zee model with Z_2 symmetry has already been excluded by neutrino experimental data [4–6]. Subsequent studies have explored flavor symmetries, including global $U(1)$ and discrete symmetries [7–10] as well as recent developments in modular flavor symmetries [11–13]. A promising new direction is the application of non-invertible symmetries, which have recently garnered significant attention in the formal and phenomenological literature.

Unlike traditional group-based symmetries, non-invertible symmetries provide selection rules that do not follow a group structure; for comprehensive reviews and applications, see [14–17] and [18–49], respectively. These selection rules from non-invertible symmetries can provide interaction structures which are not realized by invertible(group) symmetries. Furthermore, a particularly interesting feature is that such symmetries can be broken by radiative corrections even if they remain exact at the tree level; see [25, 29, 50, 51]. This scheme offers a novel conceptual framework for constructing BSM physics models and leads to unique predictions.

In this work, we investigate the application of non-invertible Z_M symmetry, denoted by Z_M^{NI} , within the Zee model framework. Remarkably Z_M^{NI} symmetry leads to a diverse set of non-invertible selection rules, which can be motivated by string theory [18]. In constructing our model, we consider a softly-broken Z_M^{NI} symmetry. We systematically classify the models in terms of transformation properties of the fields under Z_M^{NI} and identify viable candidates

by analyzing the resulting neutrino mass structures. After classification, we perform a detailed numerical analysis of a representative benchmark model, presenting predictions for neutrino sector and lepton flavor violations in charged lepton decays to illustrate the efficacy of our framework.

This paper is organized as follows. In sec. II, we discuss our framework in constructing models showing some formulas and classify models under Z_M^{NI} . In sec. III, we investigate a benchmark model and show predicted neutrino observables and lepton flavor violations. We summarize the work in sec. IV.

II. MODELS

In this section, we discuss the construction of Zee models with non-invertible Z_M symmetry. The field contents of the models are the same as the original Zee model where we introduce a second Higgs doublet Φ and $SU(2)$ singlet charged scalar field S^+ with hyper charge 1. Then we apply softly broken non-invertible Z_M symmetry, denoted by Z_M^{NI} hereafter, to the SM leptons and new scalar fields.

Under Z_M^{NI} symmetry, we assign a class $[g^k]$ for fields where g is the generator of the original Z_M discrete symmetry and k is an integer running 0 to $M - 1$ ¹. Then the products of two classes are given by

$$[g^k][g^{k'}] = [g^{k+k'}] + [g^{M-k+k'}]. \quad (1)$$

If we assign $[g^k]$ and $[g^{k'}]$ to fields ϕ and ϕ' the term $\phi\phi'$ is invariant when $[g^{k+k'}]$ or $[g^{M-k+k'}]$ coincides with trivial class $[g^0]$. This rule can be easily extended for interaction terms including three and four fields. In this work, we assign classes of Z_M^{NI} for three generations of SM leptons as $\{[g^{k_{\ell 1}}], [g^{k_{\ell 2}}], [g^{k_{\ell 3}}]\}$ to distinguish them. We also assign classes $[g^{k_\Phi}]$ and $[g^{k_S}]$ for Φ and S^+ respectively. The field contents and charge assignments are summarized in the Table I. We first show general formulas of the models and then discuss lepton flavor structure which is determined by the assignment of Z_M^{NI} .

¹ A class is defined using the automorphism such that

$$[g^k] = \{hg^kh^{-1} \mid h = e, r\} \quad (k = 0, 1, \dots, M - 1),$$

where $\{e, r\}$ is associated with gauged Z_2 symmetry on orbifold satisfying $eg^{-1}e = g$ and $rgr^{-1} = g^{-1}$. The detailed explanations can be referred to refs. [18, 19, 22]

	L_L	ℓ_R	Φ_1	Φ_2	S^+
$SU(2)_L$	2	1	2	2	1
$U(1)_Y$	$-\frac{1}{2}$	-1	$\frac{1}{2}$	$\frac{1}{2}$	1
Z_M^{NI}	$\{[g^{k_{\ell 1}}], [g^{k_{\ell 2}}], [g^{k_{\ell 3}}]\}$	$\{[g^{k_{\ell 1}}], [g^{k_{\ell 2}}], [g^{k_{\ell 3}}]\}$	$[g^{k_\Phi}]$	$[g^0]$	$[g^{k_S}]$

TABLE I: Charge assignments of the leptons and scalar fields under $SU(2)_L \otimes U(1)_Y \otimes Z_M^{NI}$.

The Yukawa interactions in lepton sector are written by

$$\mathcal{L}_{Y_\ell} = y^\ell \overline{L}_L \ell_R \Phi_2 + y^\Phi \overline{L}_L \ell_R \Phi_1 + f \overline{L}_L^c (i\sigma_2) L_L S^+ + h.c., \quad (2)$$

where σ_2 is the second Pauli matrix. Here we omitted the flavor indices and the structures of the Yukawa couplings depend on the assignment of Z_M^{NI} classes to fields as discussed below.

The scalar potential is given by

$$V = \mu_1^2 |\Phi_1|^2 + \mu_2^2 |\Phi_2|^2 - \mu_{12}^2 (\Phi_1^\dagger \Phi_2 + h.c.) + \mu (\Phi_2^T i\sigma_2 \Phi_1 S^- + h.c.) \\ + \frac{1}{2} \lambda_1 |\Phi_1|^4 + \frac{1}{2} \lambda_2 |\Phi_2|^4 + \lambda_3 |\Phi_1|^2 |\Phi_2|^2 + \lambda_4 |\Phi_1^\dagger \Phi_2|^2 + \frac{\lambda_5}{2} \{(\Phi_1^\dagger \Phi_2)^2 + h.c.\}. \quad (3)$$

In our framework, we consider Z_M^{NI} is softly broken. Then the term $\Phi_2 i\sigma_2 \Phi_1 S^-$ is always allowed in any assignment of Z_M^{NI} classes to Φ_1 and S^\pm . The assumption of soft breaking is a reasonable choice since terms forbidden by Z_M^{NI} symmetry at tree level often appear through radiative correction and mass dimensional couplings would not be suppressed.

Note that the scalar potential is the same as the original Zee model and we do not analyze it in details. In the following, we just summarize the mass eigenstates in scalar sector to calculate a neutrino mass matrix.

A. Mass eigenstates

Here we show mass eigenstates in the models and derive interactions in the mass basis. Firstly we write Higgs doublet fields in terms of the Higgs basis defined by

$$\begin{pmatrix} \Phi_1 \\ \Phi_2 \end{pmatrix} = \begin{pmatrix} c_\beta & -s_\beta \\ s_\beta & c_\beta \end{pmatrix} \begin{pmatrix} H' \\ \Phi \end{pmatrix}, \quad (4)$$

where $s_\beta = \sin \beta$ and $c_\beta = \cos \beta$ with $\tan \beta = \langle \Phi_2 \rangle / \langle \Phi_1 \rangle$. The doublet fields in the Higgs basis can be written as

$$H' = \begin{pmatrix} G^+ \\ \frac{1}{\sqrt{2}}(h'_1 + v + iG^0) \end{pmatrix}, \quad \Phi = \begin{pmatrix} H^+ \\ \frac{1}{\sqrt{2}}(h'_2 + iA) \end{pmatrix}, \quad (5)$$

where G^+ and G^0 are Namubu-Goldstone bosons absorbed by massive SM gauge bosons W^+ and Z , and $v \simeq 246$ GeV is the Higgs vacuum expectation value (VEV). The mass eigenstates for CP-even Higgs bosons are defined as

$$\begin{pmatrix} h'_1 \\ h'_2 \end{pmatrix} = \begin{pmatrix} c_{\alpha-\beta} & -s_{\alpha-\beta} \\ s_{\alpha-\beta} & c_{\alpha-\beta} \end{pmatrix} \begin{pmatrix} H \\ h \end{pmatrix} \quad (6)$$

where the mixing angle α is determined by the parameters in the Higgs potential. Here h is identified as the SM Higgs boson while H corresponds to heavy neutral CP-even one. We also write mass eigenstates of charged scalar bosons such that

$$\begin{pmatrix} H^\pm \\ S^\pm \end{pmatrix} = \begin{pmatrix} c_\chi & -s_\chi \\ s_\chi & c_\chi \end{pmatrix} \begin{pmatrix} H_1^\pm \\ H_2^\pm \end{pmatrix}, \quad (7)$$

The lepton Yukawa interactions in the scalar mass basis, with alignment limit ($s_{\alpha-\beta} = 1$), are given by

$$\begin{aligned} \mathcal{L}_{Y_\ell} = & \frac{v}{\sqrt{2}}(c_\beta y^\Phi + s_\beta y^\ell) \bar{\ell}_L \ell_R + \frac{1}{\sqrt{2}}(c_\beta y^\Phi + s_\beta y^\ell) h \bar{\ell}_L \ell_R + \frac{1}{\sqrt{2}}(s_\beta y^\Phi - c_\beta y^\ell) H \bar{\ell}_L \ell_R \\ & + \frac{i}{\sqrt{2}}(-s_\beta y^\Phi + c_\beta y^\ell) A \bar{\ell}_L \ell_R + c_\chi(-s_\beta y^\Phi + c_\beta y^\ell) H_1^+ \bar{\nu}_L \ell_R + s_\chi(s_\beta y^\Phi - c_\beta y^\ell) H_2^+ \bar{\nu}_L \ell_R \\ & + f(\bar{\nu}_L^C \ell_L - \bar{\ell}_L^C \nu_L)(s_\chi H_1^+ + c_\chi H_2^+) + h.c. \end{aligned} \quad (8)$$

The first term of RHS in Eq. (8) is a mass term of charged leptons. Thus the charged lepton mass matrix can be written by

$$M_\ell = \frac{c_\beta v}{\sqrt{2}}(y^\Phi + t_\beta y^\ell). \quad (9)$$

The mass matrix is diagonalized via mixing matrices V_R and V_L as $m_\ell \equiv \text{diag.}(m_e, m_\mu, m_\tau) = V_L^\dagger M_\ell V_R$, which are associated with transformation $\ell_{L(R)} \rightarrow V_{L(R)} \ell_{L(R)}^m$ with $\ell_{L(R)}^m$ being mass eigenstates. Therefore, the mass matrix satisfies $V_L^\dagger M_\ell M_\ell^\dagger V_L = \text{diag.}(|m_e|^2, |m_\mu|^2, |m_\tau|^2)$.

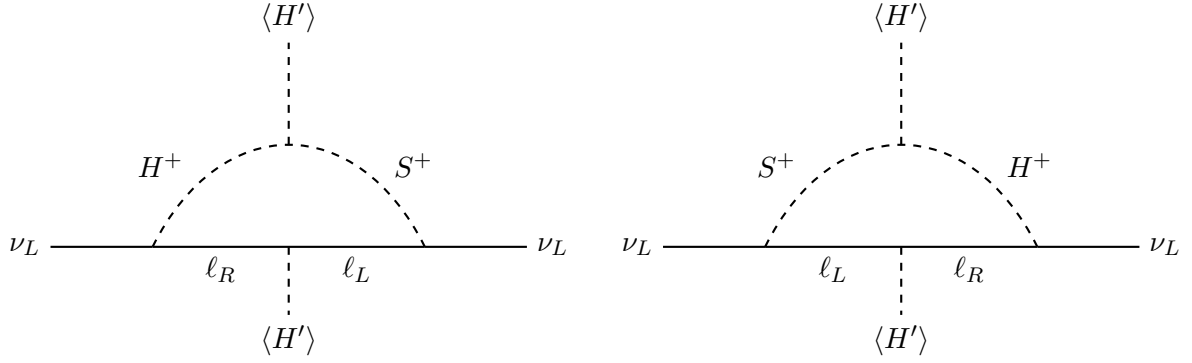


FIG. 1: One-loop diagrams inducing neutrino masses.

B. Neutrino mass

The neutrino mass matrix is generated by one-loop diagram as in the original Zee model. Neutrino masses are induced by diagrams in Fig. 1. The relevant Yukawa interactions for neutrino mass generation are written by

$$\mathcal{L}_{Y_\ell} \supset (s_\beta c_\chi H_1^+ + s_\beta s_\chi H_2^+) Y_{ij} \overline{\nu_{L_i}} \ell_{R_j}^m + (s_\chi H_1^+ + c_\chi H_2^+) F_{ij} \left(\overline{\nu_{L_i}^C} \ell_{L_j}^m - \overline{\ell_{L_i}^{mC}} \nu_{L_j} \right) + h.c., \quad (10)$$

where the relevant Yukawa couplings are given by

$$Y \equiv (-y^\Phi + \cot \beta y^\ell) V_R, \quad F \equiv f V_L. \quad (11)$$

Calculating one-loop diagrams, the neutrino mass matrix is approximately given by

$$(m_\nu)_{ij} \simeq \frac{\sin 2\chi}{16\pi^2} \ln \left(\frac{m_{H_2^+}^2}{m_{H_1^+}^2} \right) (F m_\ell Y^\dagger)_{ij} + (i \leftrightarrow j), \quad (12)$$

where charged lepton masses in the log factor are ignored.

C. Lepton flavor violation

Here we formulate charged lepton flavor violations (CLFVs). Firstly, we write Yukawa interactions relevant for CLFV in mass basis. The relevant Yukawa interactions with neutral scalar bosons are

$$\mathcal{L}_{Y_\ell} \supset (Y_h h + Y_H H - i Y_H A) \overline{\ell_L^m} \ell_R^m + h.c., \quad (13)$$

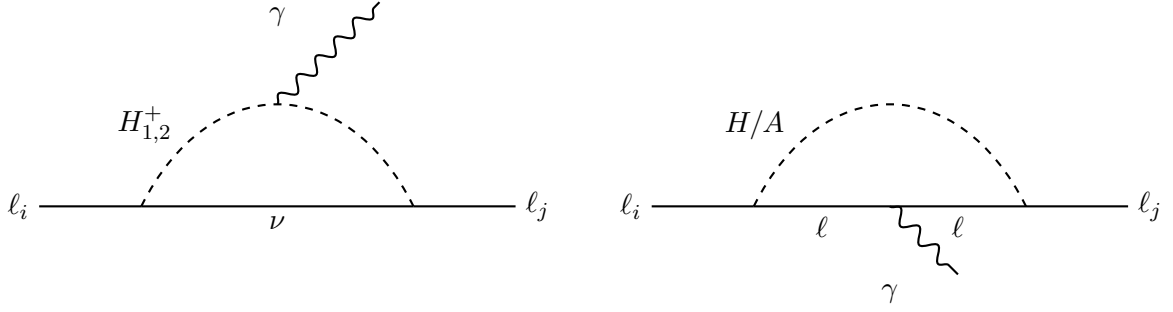


FIG. 2: One-loop diagrams inducing CLFV process $\ell_i \rightarrow \ell_j \gamma$.

where the couplings are given by

$$\begin{aligned}
 Y_h &\equiv \frac{1}{\sqrt{2}} V_L^\dagger (c_\beta y^\Phi + s_\beta y^\ell) V_R, \\
 Y_H &\equiv \frac{1}{\sqrt{2}} V_L^\dagger (s_\beta y^\Phi - c_\beta y^\ell) V_R.
 \end{aligned}
 \tag{14}$$

Note that Yukawa coupling matrix for the H and A is the same. Also Y_h should be diagonal and does not contribute to CLFV process. The relevant Yukawa interactions associated with charged scalar bosons are already given in Eq. (10) that are used to generate neutrino masses.

The CLFV decay processes, $\ell_i \rightarrow \ell_j \gamma$, are induced at one-loop level via diagrams in Fig. 2. Estimating the diagrams, we can write the branching ratio (BR) of the CLFV decay as follows

$$BR(\ell_i \rightarrow \ell_j \gamma) = \frac{48\pi^3 \alpha_{em} C_{ij}}{G_F^2} (|A_L|^2 + |A_R|^2),
 \tag{15}$$

where G_F is the Fermi constant and α_{em} is the electromagnetic fine structure constant. Here $A_{L(R)}$ can be obtained by summing up all diagrams where the detailed forms are summarized in the Appendix A; the same amplitude also induce $\mu \rightarrow e$ conversion process [52–55] where we omit to discuss the process since it is highly suppressed in our benchmark model analyzed below. Furthermore, three body CLFV decays $\ell_i^\mp \rightarrow \ell_j^\mp \ell_k^\mp \ell_l^\pm$ are induced at tree level by exchanging heavy neutral bosons via Yukawa coupling Y_H . Here we focus on $\mu \rightarrow eee$ and $\tau \rightarrow \mu\mu\mu$ CLFV processes which provides clear signal at the experiments. The BRs are then given by [3]

$$\begin{aligned}
 BR(\mu \rightarrow eee) &\simeq \frac{1}{64G_F^2 m_H^4} [|(Y_H)_{11}^*(Y_H)_{12}|^2 + |(Y_H)_{11}(Y_H)_{21}^*|^2] BR(\mu \rightarrow e\nu\bar{\nu}), \\
 BR(\tau \rightarrow \mu\mu\mu) &\simeq \frac{1}{64G_F^2 m_H^4} [|(Y_H)_{22}^*(Y_H)_{23}|^2 + |(Y_H)_{22}(Y_H)_{32}^*|^2] BR(\tau \rightarrow \mu\nu\bar{\nu}),
 \end{aligned}
 \tag{16}$$

where we ignored charged lepton masses and took $m_A = m_H$. The current upper bounds are given by [56–61]

$$\begin{aligned} BR(\mu \rightarrow e\gamma) &< 1.5 \times 10^{-13}, & BR(\tau \rightarrow e\gamma) &< 3.3 \times 10^{-8}, & BR(\tau \rightarrow \mu\gamma) &< 4.2 \times 10^{-8} \\ BR(\mu \rightarrow eee) &< 1.0 \times 10^{-12}, & BR(\tau \rightarrow \mu\mu\mu) &< 2.1 \times 10^{-8}. \end{aligned} \quad (17)$$

We impose these constraints in numerical analysis.

D. Exploring viable models

In this subsection, we explore viable models. The models are classified by the assignments of Z_M classes to the fields in Table I. The structures of Yukawa couplings f and y^Φ are then determined by the choice of the assignment of classes. Note that the Yukawa coupling matrix y^ℓ is diagonal, since we assign the same classes for L_L and ℓ_R , and Φ_2 has no charge under Z_M^{NI} .

For illustration, we investigate a simple case under Z_4^{NI} . In the first example, three generations of SM leptons are assigned to have $\{[g^0], [g^1], [g^2]\}$ classes, and both Φ_1 and S^+ belong to the class $[g^1]$. The structure of Yukawa couplings are

$$f : \begin{pmatrix} 0 & \times & 0 \\ \times & 0 & \times \\ 0 & \times & 0 \end{pmatrix}, \quad y^\Phi : \begin{pmatrix} 0 & \times & 0 \\ \times & 0 & \times \\ 0 & \times & 0 \end{pmatrix}, \quad (\text{example 1}) \quad (18)$$

where "×" indicates a non-zero component. For example, $\overline{(L_L)_1}(\ell_R)_1\Phi_1$ is not allowed since the products of classes $[g^0][g^0][g^1]$ does not contain trivial class $[g^0]$. The other components can be also understood in the same manner.

The structure of neutrino mass is determined by the products of matrices $Fm_\ell Y^\dagger = fM_\ell(-y^\Phi + \cot\beta y^\ell)^\dagger$ and its transpose. Then structure of m_ν in this case is

$$m_\nu : \begin{pmatrix} \times & \times & \times \\ \times & \times & \times \\ \times & \times & \times \end{pmatrix}, \quad m_\nu : \begin{pmatrix} \times & 0 & \times \\ 0 & \times & 0 \\ \times & 0 & \times \end{pmatrix} \quad (t_\beta \rightarrow \infty), \quad (\text{example 1}) \quad (19)$$

where we show the structure for the limit of $t_\beta \rightarrow \infty$ as a reference. Thus, we do not have specific structure for finite t_β while two-zero structure appears in the limit $t_\beta \rightarrow \infty$;

this two-zero structure cannot fit neutrino data. As the second example, we set the same assignments for SM leptons, while assignment of class for $\Phi_1(S^+)$ is chosen to be $[g^1]([g^2])$. In this example, structure of f is the same but that of y^Φ is changed to be

$$y^\Phi : \begin{pmatrix} 0 & 0 & \times \\ 0 & \times & 0 \\ \times & 0 & 0 \end{pmatrix}, \quad (\text{example 2}). \quad (20)$$

Then the structure of neutrino mass becomes

$$m_\nu : \begin{pmatrix} 0 & \times & 0 \\ \times & 0 & \times \\ 0 & \times & 0 \end{pmatrix}, \quad (\text{example 2}) \quad (21)$$

where it does not change in the $t_\beta \rightarrow \infty$ limit. Thus, in this example, we can not fit the neutrino data due to the structure.

As in the examples, the assignments of classes to fields in the models determine the structure of the neutrino mass matrix. Then we explore viable models for Z_M with $M = 4$ to $M = 7$ where $M = 4$ is the minimal choice to distinguish three generations by three classes. We also impose following conditions,

- Assignments of classes to L_L and ℓ_R are the same so that y^ℓ matrix is always diagonal,
- The SM quarks and Φ_2 belong to the trivial class $[g^0]$ so that quarks only couple to Φ_2 without restricting structure of Yukawa couplings to realize quark masses and mixings.

Under these conditions, structures of neutrino mass matrix are examined for different assignments of Z_M^{NI} classes to the fields for each M . Then we list viable models providing a structure of neutrino mass which is possible to fit the neutrino data. The complete lists of viable models for each M are shown in the appendix B.

III. NUMERICAL ANALYSIS OF A BENCHMARK MODEL

In this section, we carry out numerical analysis for our benchmark model. As a benchmark model, we choose Z_7^{NI} model (1) in Table VI where the assignment is given in Table II.

	L_L	ℓ_R	Φ_1	Φ_2	S^+
$SU(2)_L$	$\mathbf{2}$	$\mathbf{1}$	$\mathbf{2}$	$\mathbf{2}$	$\mathbf{1}$
$U(1)_Y$	$-\frac{1}{2}$	-1	$\frac{1}{2}$	$\frac{1}{2}$	1
Z_7^{NI}	$\{[g^0], [g^1], [g^2]\}$	$\{[g^0], [g^1], [g^2]\}$	$[g^3]$	$[g^0]$	$[g^1]$

TABLE II: Charge assignments for our benchmark model under $SU(2)_L \otimes U(1)_Y \otimes Z_7^{NI}$.

A. Description of the benchmark model

In the model structures of Yukawa couplings are

$$y^\ell : \begin{pmatrix} y_{11}^\ell & 0 & 0 \\ 0 & y_{22}^\ell & 0 \\ 0 & 0 & y_{33}^\ell \end{pmatrix}, \quad y^\Phi : \begin{pmatrix} 0 & 0 & 0 \\ 0 & 0 & y_{23}^\Phi \\ 0 & y_{32}^\Phi & y_{33}^\Phi \end{pmatrix}, \quad f : \begin{pmatrix} 0 & f_{12} & 0 \\ -f_{12} & 0 & f_{23} \\ 0 & -f_{23} & 0 \end{pmatrix}, \quad (22)$$

where we explicitly write the components of the matrices. Thus, charged lepton mass matrix becomes

$$\begin{aligned} M_\ell &= \frac{vs_\beta}{\sqrt{2}} (\cot \beta y^\Phi + y^\ell) \\ &= \frac{vs_\beta}{\sqrt{2}} \left[\cot \beta \begin{pmatrix} 0 & 0 & 0 \\ 0 & 0 & y_{23}^\Phi \\ 0 & y_{32}^\Phi & y_{33}^\Phi \end{pmatrix} + \begin{pmatrix} y_{11}^\ell & 0 & 0 \\ 0 & y_{22}^\ell & 0 \\ 0 & 0 & y_{33}^\ell \end{pmatrix} \right]. \end{aligned} \quad (23)$$

In this case, the first generation of charged lepton does not mix with other generations, and the mixing matrix $V_{L(R)}$ has the structure of

$$V_{L(R)} : \begin{pmatrix} 1 & 0 & 0 \\ 0 & \times & \times \\ 0 & \times & \times \end{pmatrix}. \quad (24)$$

The electron mass is simply given by $m_e = vs_\beta y_{11}^\ell / \sqrt{2}$, which fixes the coupling y_{11}^ℓ . The mixing matrix $V_{L(R)}$ is calculated by numerically diagonalizing the mass matrix in the analysis below. We also note that CLFV associated with electron is highly suppressed due to the structure of the Yukawa couplings.

The neutrino mass is given by Eq. (24) and its structure is

$$m_\nu : \begin{pmatrix} 0 & \times & \times \\ \times & \times & \times \\ \times & \times & \times \end{pmatrix}, \quad m_\nu|_{t_\beta \rightarrow \infty} : \begin{pmatrix} 0 & 0 & \times \\ 0 & \times & \times \\ \times & \times & \times \end{pmatrix}, \quad (25)$$

where $m_\nu|_{t_\beta \rightarrow \infty}$ corresponds to the mass matrix under the $t_\beta \rightarrow \infty$ limit. An interesting point of the model is that we have one-zero texture with finite t_β while two-zero texture is realized in the limit of $t_\beta \rightarrow \infty$ representing significant dependence of neutrino mass matrix to t_β value. We thus numerically explore the neutrino observables for different t_β values below.

The mass eigenvalues for active neutrinos are obtained by diagonalizing the mass matrix as $D_\nu \equiv V_\nu^T m_\nu V_\nu$ where $D_\nu = \{D_{\nu_1}, D_{\nu_2}, D_{\nu_3}\}$. The neutrino mixing are described by the standard parametrization in terms of the Pontecorvo-Maki-Nakagawa-Sakata (PMNS) mixing matrix U defined by $U \equiv V_{eL}^\dagger V_\nu$, and the Majorana phase is defined by $[1, e^{i\alpha_{21}/2}, e^{i\alpha_{31}/2}]$ [62]. Then, we estimate the Majorana phases using the formulas;

$$\cos\left(\frac{\alpha_{21}}{2}\right) = \frac{\text{Re}[U_{e1}^* U_{e2}]}{c_{12}s_{12}c_{13}^2}, \quad \cos\left(\frac{\alpha_{31}}{2} - \delta_{CP}\right) = \frac{\text{Re}[U_{e1}^* U_{e3}]}{c_{12}s_{13}c_{13}}, \quad (26)$$

$$\sin\left(\frac{\alpha_{21}}{2}\right) = \frac{\text{Im}[U_{e1}^* U_{e2}]}{c_{12}s_{12}c_{13}^2}, \quad \sin\left(\frac{\alpha_{31}}{2} - \delta_{CP}\right) = \frac{\text{Im}[U_{e1}^* U_{e3}]}{c_{12}s_{13}c_{13}}, \quad (27)$$

where $c_{ij}(s_{ij})$ stands for $\cos\theta_{ij}(\sin\theta_{ij})$ with θ_{ij} being the mixing angle in the PMNS matrix. In deriving phases, $\alpha_{21}/2$ and $\frac{\alpha_{31}}{2} - \delta_{CP}$ are subtracted from π , if $\cos(\alpha_{21}/2)$ and $\cos\left(\frac{\alpha_{31}}{2} - \delta_{CP}\right)$ are negative. The Dirac CP-phase δ_{CP} is given by

$$\cos\delta_{CP} = \frac{-1}{2c_{12}s_{12}c_{23}s_{23}s_{13}} (|U_{31}|^2 - s_{12}^2 s_{23}^2 - c_{12}^2 c_{23}^2 s_{13}^2), \quad (28)$$

$$\sin\delta_{CP} = \frac{1}{s_{23}c_{23}s_{12}c_{12}s_{13}c_{13}^2} \text{Im}[U_{11}U_{22}U_{12}^*U_{21}^*]. \quad (29)$$

For convenience, we rewrite the neutrino mass matrix as $m_\nu \equiv \kappa \tilde{m}_\nu$ where the factor $\kappa \equiv \sin 2\chi$ is used to scale the neutrino mass. Therefore, κ can be determined in terms of rescaled neutrino mass eigenvalues $\tilde{D}_\nu (\equiv D_\nu/\kappa)$ and atmospheric neutrino mass-squared difference Δm_{atm}^2 such that

$$\text{(NH)} : \kappa^2 = \frac{|\Delta m_{\text{atm}}^2|}{\tilde{D}_{\nu_3}^2 - \tilde{D}_{\nu_1}^2}, \quad \text{(IH)} : \kappa^2 = \frac{|\Delta m_{\text{atm}}^2|}{\tilde{D}_{\nu_2}^2 - \tilde{D}_{\nu_3}^2}, \quad (30)$$

where NH and IH stand for the normal and inverted hierarchies, respectively. Subsequently, the solar neutrino mass-squared difference is obtained by the relation

$$\Delta m_{\text{sol}}^2 = \kappa^2 (\tilde{D}_{\nu_2}^2 - \tilde{D}_{\nu_1}^2). \quad (31)$$

The effective mass for neutrino double beta decay, m_{ee} , is written by

$$m_{ee} = \kappa \left| \tilde{D}_{\nu_1} \cos^2 \theta_{12} \cos^2 \theta_{13} + \tilde{D}_{\nu_2} \sin^2 \theta_{12} \cos^2 \theta_{13} e^{i\alpha_{21}} + \tilde{D}_{\nu_3} \sin^2 \theta_{13} e^{i(\alpha_{31} - 2\delta_{\text{CP}})} \right|. \quad (32)$$

The strongest upper bounds are given by the KamLAND-Zen experiment [63]. The upper bound on m_{ee} at the 90% CL is

$$m_{ee} \leq (28 - 122) \text{ meV}, \quad (33)$$

where the range is due to the different method to estimate nuclear matrix elements. Future experiments can provide stronger constraints such that $m_{ee} < (9 - 21) \text{ meV}$ by LEGEND-1000 [64] and $m_{ee} \leq (4.7 - 20.3) \text{ meV}$ by mEXO [65].

In addition, we also consider direct search for neutrino mass where the model independent observable is $m_{\nu_e}^2 \equiv \kappa^2 \sum_i \tilde{D}_{\nu_i}^2 |U_{ei}|^2$. The current limit, at 90% CL, by KATRIN [66] is

$$m_{\nu_e} \leq 450 \text{ meV}. \quad (34)$$

In numerical analysis, we also take into account the cosmological bounds on the sum of neutrino mass $\sum D_\nu$. The upper bound is $\sum D_\nu \leq 120 \text{ meV}$ from Planck data with standard ΛCDM cosmological model [67]. More stringent constraint is given by combining baryon acoustic oscillation (BAO) data from DESI and CMB data leading the upper bound on the sum as $\sum D_\nu \leq 72 \text{ meV}$ [68].

B. Numerical analysis

We numerically analyze the lepton mass matrices for the benchmark model adopting the formulas in previous subsection. Originally, we have 8 Yukawa couplings

$$\{y_{11}^\ell, y_{22}^\ell, y_{33}^\ell, y_{23}^\Phi, y_{32}^\Phi, y_{33}^\Phi, f_{12}, f_{23}\}, \quad (35)$$

where we choose $\{y_{11}^\ell, y_{22}^\ell, y_{33}^\ell\}$ to be real parameters using phase redefinition for lepton fields. Then the couplings $\{y_{11}^\ell, y_{22}^\ell, y_{33}^\ell\}$ are fixed to fit charged lepton masses. For estimating

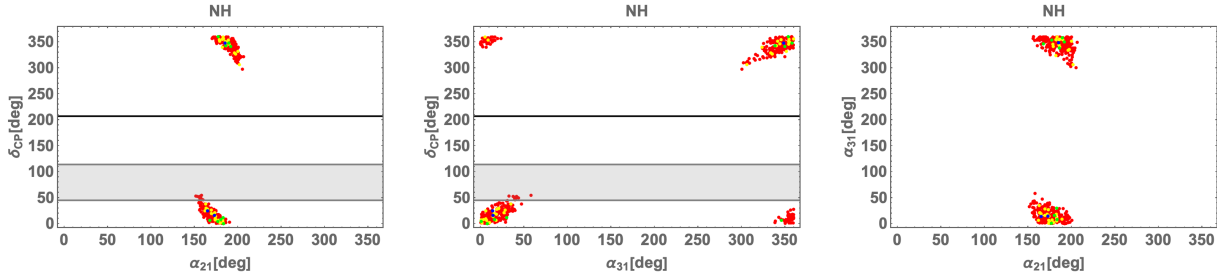


FIG. 3: Predicted values for neutrino observables from allowed parameter points on α_{21} - δ_{CP} (left), α_{31} - δ_{CP} (center) and α_{21} - α_{31} (right) plane for $\tan \beta = 1$. The color of points indicates an estimated χ^2 value providing 0-1 σ (blue), 1-2 σ (green), 2-3 σ (yellow) and 3-5 σ (red) deviations; indications of color of points are common in the figures afterwards. In the left and center plots the gray region indicate the value of δ_{CP} is deviated more than 3 σ in NuFit 6.1 while the horizontal black line represents the best fit value of δ_{CP} ; they are common in the plots below showing the δ_{CP} .

neutrino observables, we scan remaining free parameters as follows

$$|y_{23,32,33}^{\Phi}| \in [10^{-6}, 10^{-2}], \quad |f_{12,23}| \in [10^{-6}, 0.1], \quad (36)$$

where the complex phases of the couplings are scanned within $[-\pi, \pi]$. Here we take $|y_{23,32,33}^{\Phi}|$ to be less than 10^{-2} since larger values of these couplings spoil to fit charged lepton masses for $t_{\beta} = 1$. In our analysis, we consider the cases of $t_{\beta} = 1, 100$ and 10000 as reference values for illustration. We then carry out chi-square analysis estimating the $\Delta\chi^2$ value of

$$\Delta\chi^2 = \sum_i \left(\frac{O_i^{\text{obs}} - O_i^{\text{th}}}{\delta O_i^{\text{exp}}} \right)^2, \quad (37)$$

where $O_i^{\text{obs(th)}}$ is the observed (theoretically) obtained value of the observables and δO_i^{exp} denotes the experimental error of 1 σ level. In the fitting, we take into account the neutrino observables $\{\sin^2 \theta_{12}, \sin^2 \theta_{13}, \sin^2 \theta_{23}, \Delta m_{\text{atm}}^2, \Delta m_{\text{sol}}^2\}$ with global fit of NuFit 6.1 [69]. The other neutrino observables are estimated as output values such as CP-phases.

In the followings, we summarize the results of our numerical analysis showing predictions for neutrino observables and CLFV BRs. Firstly, we find no allowed parameters which can fit neutrino masses and mixing angles in the IH case. We thus show our results in NH case for different $\tan \beta$ values below.

(i) Results of $t_{\beta} = 1$ case

Fig. 3 shows the predictions regarding Dirac and Majorana CP phases where each point

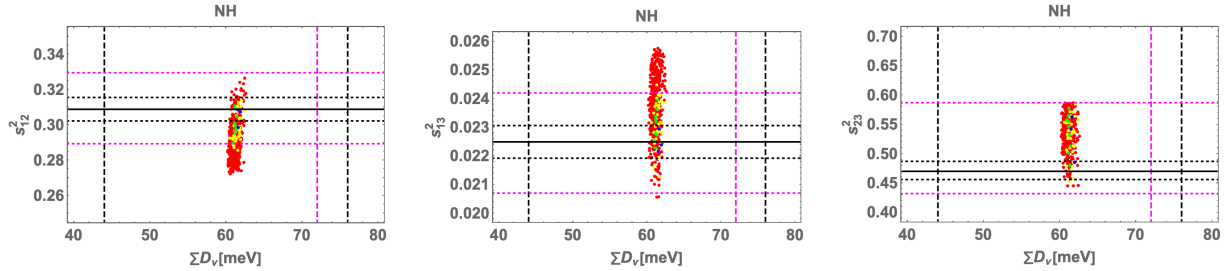


FIG. 4: Predicted values for neutrino observables from allowed parameter points on $\sum D_\nu$ - s_{12}^2 (left), $\sum D_\nu$ - s_{13}^2 (center) and $\sum D_\nu$ - s_{23}^2 (right) plane for $\tan\beta = 1$. The region between horizontal black(magenta) lines corresponding to the $1\sigma(3\sigma)$ range. The vertical magenta dashed line indicate the upper limit of $\sum D_\nu$ by Planck+DESI data while the region between vertical black dashed lines can be tested by future CMB observations. The lines are common in the plots below showing mixing angles and $\sum m_\nu$.

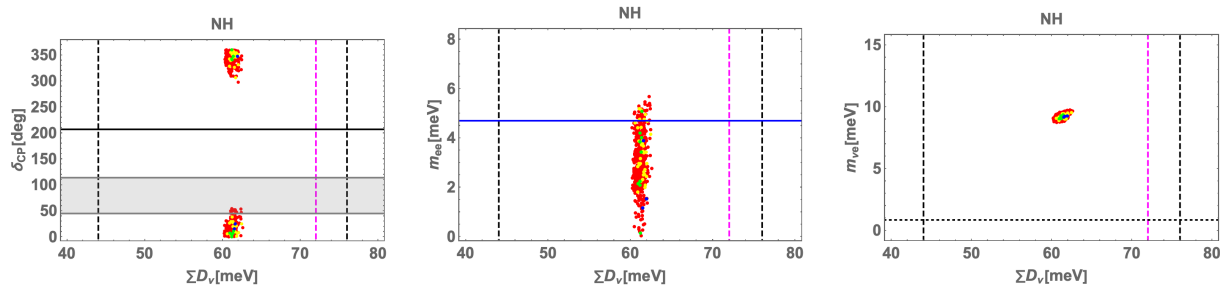


FIG. 5: Predicted values for neutrino observables from allowed parameter points on $\sum D_\nu$ - δ_{CP} (left), $\sum D_\nu$ - m_{ee} (center) and $\sum D_\nu$ - $m_{\nu e}$ (right) plane for $\tan\beta = 1$. The blue horizontal line in the center plot corresponds to the strongest future sensitivity by mEXO; it is common in the other plots below.

corresponds to one allowed parameter sets and its color indicates an estimated χ^2 value providing 0 - 1σ (blue), 1 - 2σ (green), 2 - 3σ (yellow) and 3 - 5σ (red) deviations; indications of color of points are common in the figures afterwards. The left, center and right plots in Fig. 3 represent correlations on α_{21} - δ_{CP} , α_{31} - δ_{CP} and α_{21} - α_{31} plane, respectively. In the left and center plots the gray region indicate the value of δ_{CP} is deviated more than 3σ in NuFit 6.1 while the horizontal black line represents the best fit value of δ_{CP} . We find that the value of δ_{CP} is preferred to be within 0 - 50 [deg] and 300 - 360 [deg] region. On the other hand,

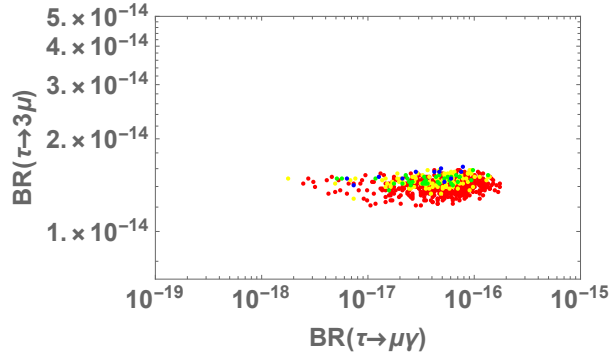


FIG. 6: The predicted BRs of CLFV processes $\tau \rightarrow \mu\gamma$ and $\tau \rightarrow 3\mu$.

the Majorana phase $\alpha_{21(31)}$ is predicted to be within around 150-205 [deg] (0-60 and 300-360 [deg]).

Fig. 4 shows our predictions on $\sum D_\nu - s_{12}^2$ (left), $\sum D_\nu - s_{13}^2$ (center) and $\sum D_\nu - s_{23}^2$ (right) planes. The sum of neutrino masses is concentrated around 60-62 meV that is below the current cosmological limit. For mixing angles, we find points in most of the region within 3σ level. The region between horizontal black(magenta) lines corresponding to the $1\sigma(3\sigma)$ range. The vertical magenta dashed line indicate the upper limit of $\sum D_\nu$ by Planck+DESI data while the region between vertical black dashed lines can be tested by future CMB observations [70–72]. The lines are common in the plots below showing mixing angles and $\sum m_\nu$.

Fig. 5 shows the predicted region on $\sum D_\nu - \delta_{CP}$ (left), $\sum D_\nu - m_{ee}$ (center) and $\sum D_\nu - m_{\nu_e}$ (right) planes. We find the range of m_{ee} is $m_{ee} \lesssim 5.5$ meV. The region for m_{ν_e} is localized around $m_{\nu_e} \sim 9$ -10 meV. The blue horizontal line in the center plot corresponds to the strongest future sensitivity by mEXO; it is common in the other plots below. .

Fig. 6 shows our prediction regarding CLFV BRs where we show $BR(\tau \rightarrow \mu\gamma)$ and $BR(\tau \rightarrow 3\mu)$ since the other BRs are forbidden or highly suppressed in the model due to the structure of the Yukawa matrices. We find that the value of $BR(\tau \rightarrow 3\mu)$ is concentrated around 1.5×10^{-14} while $BR(\tau \rightarrow \mu\gamma)$ has the range around $[2 \times 10^{-18}, 2 \times 10^{-16}]$. These values of BRs are sufficiently below the current bounds, and we do not find clear correlation for them.

(ii) Results of $t_\beta = 100$ case

Fig. 7 shows the predictions regarding Dirac and Majorana CP phases where the left, center

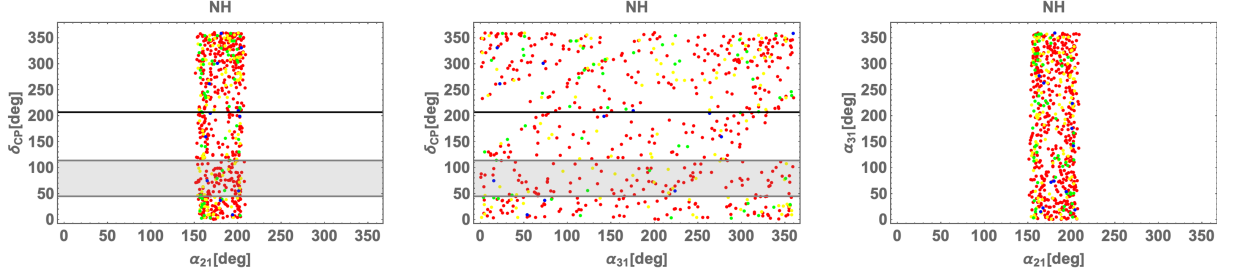


FIG. 7: Predicted values for neutrino observables from allowed parameter points on α_{21} - δ_{CP} (left), α_{31} - δ_{CP} (center) and α_{21} - α_{31} (right) plane for $\tan\beta = 100$.

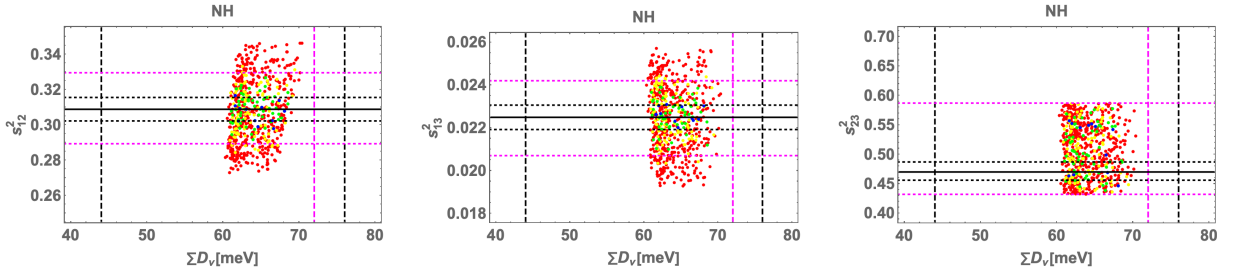


FIG. 8: Predicted values for neutrino observables from allowed parameter points on $\sum D_\nu$ - s_{12}^2 (left), $\sum D_\nu$ - s_{13}^2 (center) and $\sum D_\nu$ - s_{23}^2 (right) plane for $\tan\beta = 100$.

and right plots in Fig. 7 represents correlations on α_{21} - δ_{CP} , α_{31} - δ_{CP} and α_{21} - α_{31} plane, respectively. We find that the value of α_{21} is restricted within around 150-200 [deg]. On the other hand, the other phases δ_{CP} and α_{32} can be any value. We also do not find any correlation among the phases.

Fig. 8 shows our predictions on $\sum D_\nu$ - s_{12}^2 (left), $\sum D_\nu$ - s_{13}^2 (center) and $\sum D_\nu$ - s_{23}^2 (right) planes. The predicted range of sum of neutrino masses is around 60-69 meV that is below the current cosmological limit. For mixing angles, we find points in most of the region within 3σ level.

Fig. 9 shows the predicted region on $\sum D_\nu$ - δ_{CP} (left), $\sum D_\nu$ - m_{ee} (center) and $\sum D_\nu$ - m_{ν_e} (right) planes. We find the range of m_{ee} is $m_{ee} \lesssim 9$ meV and a little correlation between $\sum D_\nu$ and m_{ee} . The region for m_{ν_e} is within around 8-12 meV where we find some correlation between $\sum D_\nu$ and m_{ν_e} .

Fig. 10 shows our prediction regarding CLFV BRs for $\tau \rightarrow \mu\gamma$ and $BR(\tau \rightarrow 3\mu)$. We find the range of these BRs as around $BR(\tau \rightarrow \mu\gamma) \in [10^{-23}, 10^{-16}]$ and $BR(\tau \rightarrow 3\mu) \in$

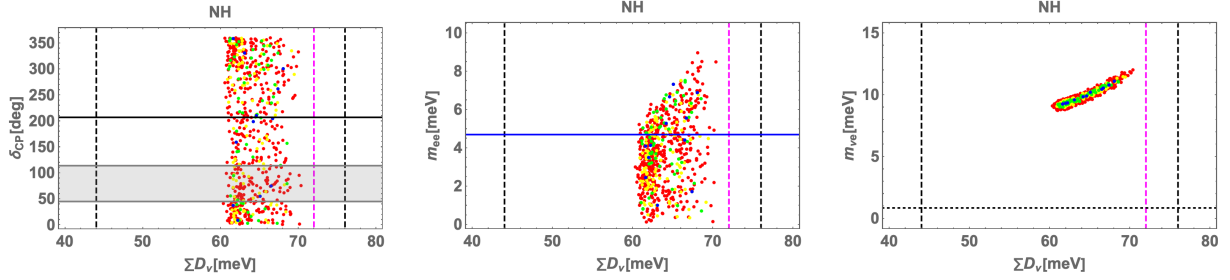


FIG. 9: Predicted values for neutrino observables from allowed parameter points on $\sum D_\nu$ - δ_{CP} (left), $\sum D_\nu$ - m_{ee} (center) and $\sum D_\nu$ - $m_{\nu e}$ (right) plane for $\tan\beta = 100$.

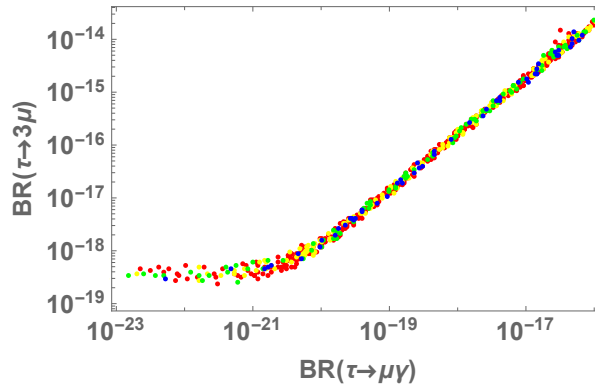


FIG. 10: The predicted BRs of CLFV processes $\tau \rightarrow \mu\gamma$ and $\tau \rightarrow 3\mu$.

$[10^{-19}, 10^{-14}]$. In addition, we find clear correlation between these BRs.

(iii) Results of $t_\beta = 10000$ case

Fig. 11 shows the predictions regarding Dirac and Majorana CP phases where the left, center and right plots in Fig. 11 represents correlations on α_{21} - δ_{CP} , α_{31} - δ_{CP} and α_{21} - α_{31} plane, respectively. We find that the value of α_{21} is restricted within around 150-200 [deg] while δ_{CP} and α_{31} can be any values. We also find some correlations between δ_{CP} and $\alpha_{21(31)}$ as shown in the left(center) plot while there is no correlation between α_{21} and α_{31} .

Fig. 12 shows our predictions on $\sum D_\nu$ - s_{12}^2 (left), $\sum D_\nu$ - s_{13}^2 (center) and $\sum D_\nu$ - s_{23}^2 (right) planes. The predicted range of sum of neutrino masses is around 60-70 meV that is below the current cosmological limit, and we find points in most of the region within 3σ level for mixing angles. The results are similar to $t_\beta = 100$ case.

Fig. 13 shows the predicted region on $\sum D_\nu$ - δ_{CP} (left), $\sum D_\nu$ - m_{ee} (center) and $\sum D_\nu$ - $m_{\nu e}$ (right) planes. We find the predicted range of these values similar to the case of $t_\beta = 100$;

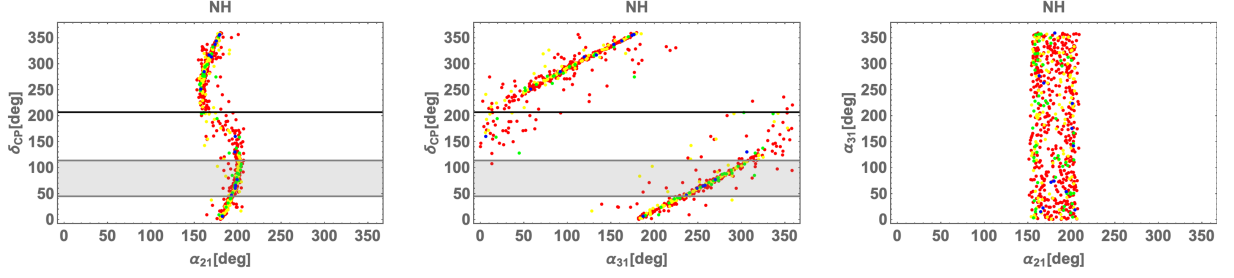


FIG. 11: Predicted values for neutrino observables from allowed parameter points on α_{21} - δ_{CP} (left), α_{31} - δ_{CP} (center) and α_{21} - α_{31} (right) plane for $\tan\beta = 10000$.

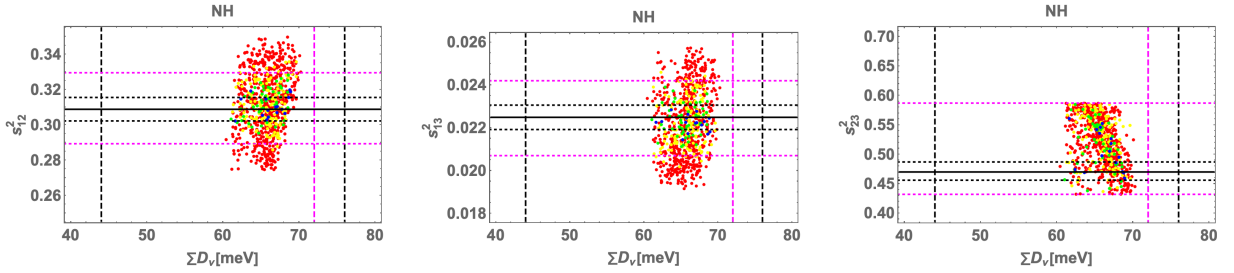


FIG. 12: Predicted values for neutrino observables from allowed parameter points on $\sum D_\nu$ - s_{12}^2 (left), $\sum D_\nu$ - s_{13}^2 (center) and $\sum D_\nu$ - s_{23}^2 (right) plane for $\tan\beta = 10000$.

$m_{ee} \lesssim 9$ meV and m_{ν_e} is within around 8-12 meV. On the other hand, we have some correlations between $\sum D_\nu$ - δ_{CP} and $\sum D_\nu$ - m_{ν_e} in this case in contrast to the $t_\beta = 100$ case.

Fig. 14 shows our prediction regarding CLFV BRs for $\tau \rightarrow \mu\gamma$ and $BR(\tau \rightarrow 3\mu)$. We find the range of these BRs as around $BR(\tau \rightarrow \mu\gamma) \in [10^{-26}, 10^{-16}]$ and $BR(\tau \rightarrow 3\mu) \in [10^{-24}, 10^{-14}]$. In addition, we find clear correlation between these BRs.

Qualitative characteristic of $\tan\beta$ dependence: Here we discuss the dependence of our predictions on $\tan\beta$. For $\tan\beta = 1$ case, y^Φ and y^ℓ equally contribute to M_ℓ and Y . In this case, charged lepton mass value strongly affects neutrino mass matrix and the restriction to neutrino observables are stronger than other cases as we see in Figs. 3-5. For $\tan\beta = 100$ case, the larger $\tan\beta$ value mildly suppresses $y^\Phi(y^\ell)$ contribution to $M_\ell(Y)$. In this case, neutrino observables are less restricted and we don't have predictions for CP phases as shown in Figs. 7-9. For $\tan\beta = 10000$ case, M_ℓ becomes almost diagonal and the neutrino mass matrix is close to two-zero texture one. We then have some correlations in neutrino observables such as CP phases and masses as shown in Figs. 11-13.

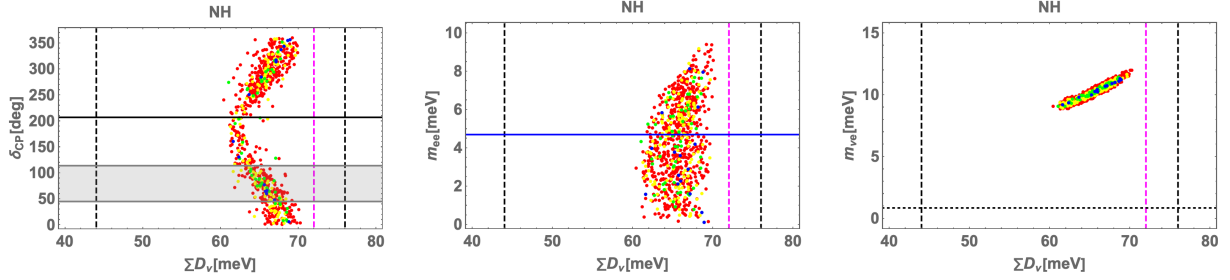


FIG. 13: Predicted values for neutrino observables from allowed parameter points on $\sum D_\nu$ - δ_{CP} (left), $\sum D_\nu$ - m_{ee} (center) and $\sum D_\nu$ - $m_{\nu e}$ (right) plane for $\tan\beta = 10000$.

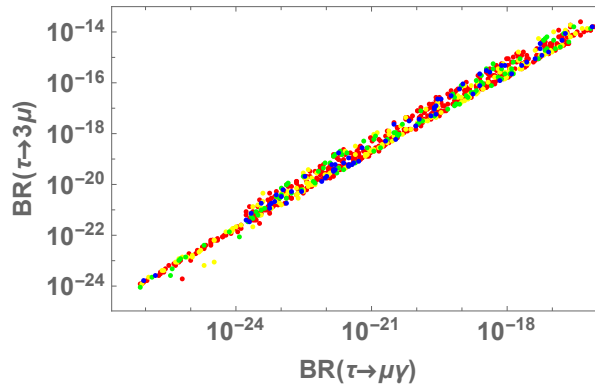


FIG. 14: The predicted BRs of CLFV processes $\tau \rightarrow \mu\gamma$ and $\tau \rightarrow 3\mu$.

Furthermore, the model would be tested by exploring signals of heavy scalar productions. In particular, exotic neutral scalars can decay violating lepton flavor as $H/A \rightarrow \ell^+ \ell'^-$. These signals can be explored by the current and future experimental energy that can be realized by the LHC, FCC [73, 74], CEPC [75–77] and muon colliders [78, 79]. Detailed study of collider signals is beyond the scope of this paper and left as future works.

IV. SUMMARY AND DISCUSSION

In this work, we have investigated Zee models incorporating with non-invertible symmetry Z_M^{NI} . The introduction of Z_M^{NI} provides novel non-invertible selection rules that leads to specific Yukawa coupling structures, which are unattainable through traditional group-symmetric approaches. We have systematically classified these models in terms of assignments of classes to fields under Z_M^{NI} for $M = 4$ to $M = 7$. By scrutinizing the resulting

neutrino mass matrices, we have identified a set of viable models that are consistent with the current neutrino oscillation data.

Following this classification, we have explored a benchmark model based on Z_7^{NI} symmetry. We have found that the neutrino mass matrix exhibits either one-zero or two-zero texture, depending on the value of $\tan\beta$. Our numerical results demonstrate that predictions for neutrino observables and charged lepton flavor violating processes, such as $\tau \rightarrow 3\mu$, are highly sensitive to the $\tan\beta$ parameter. The analysis of the benchmark model illustrates the unique phenomenological features of Zee model under Z_M^{NI} . Given the distinctive signatures identified in this study, we expect these models to be rigorously tested by upcoming high-precision neutrino experiments and searches for lepton flavor violations.

Acknowledgments

The project is supported by the Fundamental Research Funds for the Central Universities (T. N.) and Zhongyuan Talent (Talent Recruitment Series) Foreign Experts Project (H. O.).

Appendix A: Amplitudes for CLFVs

Here we summarize the formulas for decay amplitudes of the CLFV decays $\ell_i \rightarrow \ell_j \gamma$. The amplitude $A_{L(R)}$ in Eq. (15) is written as the sum of contributions associated with different scalar bosons, $\{h, H, A, H_{1,2}^\pm\}$, such that

$$A_{L(R)} = \sum_{\phi^0=h,H,A} A_{L(R)}^{\phi^0} + A_{L(R)}^{H_1^\pm} + A_{L(R)}^{H_2^\pm}. \quad (\text{A1})$$

Neutral scalar contributions in Eq. (A1) are written by

$$\begin{aligned} \left(A_L^{\phi^0}\right)_{ji} = \frac{1}{16\pi^2 m_i} & \left[(Y_{\phi^0}^\dagger)_{jk} (Y_{\phi^0})_{ki} m_i I_1(m_i, m_j, m_k, m_{\phi^0}) + (Y_{\phi^0})_{jk} (Y_{\phi^0}^\dagger)_{ki} m_j I_2(m_i, m_j, m_k, m_{\phi^0}) \right. \\ & \left. + \eta (Y_{\phi^0}^\dagger)_{jk} (Y_{\phi^0}^\dagger)_{ki} m_k I_3(m_i, m_j, m_k, m_{\phi^0}) \right] \end{aligned} \quad (\text{A2})$$

$$\begin{aligned} \left(A_R^{\phi^0}\right)_{ji} = \frac{1}{16\pi^2 m_i} & \left[(Y_{\phi^0}^\dagger)_{jk} (Y_{\phi^0})_{ki} m_j I_2(m_i, m_j, m_k, m_{\phi^0}) + (Y_{\phi^0})_{jk} (Y_{\phi^0}^\dagger)_{ki} m_i I_1(m_i, m_j, m_k, m_{\phi^0}) \right. \\ & \left. + \eta (Y_{\phi^0})_{jk} (Y_{\phi^0})_{ki} m_k I_3(m_i, m_j, m_k, m_{\phi^0}) \right], \end{aligned} \quad (\text{A3})$$

where $\eta = +1$ for $\phi^0 = h, H$ and -1 for $\phi^0 = A$.

$$(A_L^{H_1^+})_{ji} = \frac{-1}{16\pi^2 m_i} \left[(Y_{H_1^+}^\dagger)_{jk} (Y_{H_1^+})_{ki} m_i I_4(m_i, m_j, m_{H_1^+}) + (F_1^\dagger)_{jk} (F_1)_{ki} m_j I_5(m_i, m_j, m_{H_1^+}) \right], \quad (\text{A4})$$

$$(A_L^{H_2^+})_{ji} = \frac{-1}{16\pi^2 m_i} \left[(Y_{H_2^+}^\dagger)_{jk} (Y_{H_2^+})_{ki} m_i I_4(m_i, m_j, m_{H_2^+}) + (F_2^\dagger)_{jk} (F_2)_{ki} m_j I_5(m_i, m_j, m_{H_2^+}) \right], \quad (\text{A5})$$

$$(A_R^{H_1^+})_{ji} = \frac{-1}{16\pi^2 m_i} \left[(Y_{H_1^+}^\dagger)_{jk} (Y_{H_1^+})_{ki} m_j I_5(m_i, m_j, m_{H_1^+}) + (F_1^\dagger)_{jk} (F_1)_{ki} m_i I_4(m_i, m_j, m_{H_1^+}) \right], \quad (\text{A6})$$

$$(A_R^{H_2^+})_{ji} = \frac{-1}{16\pi^2 m_i} \left[(Y_{H_2^+}^\dagger)_{jk} (Y_{H_2^+})_{ki} m_j I_5(m_i, m_j, m_{H_2^+}) + (F_2^\dagger)_{jk} (F_2)_{ki} m_i I_4(m_i, m_j, m_{H_2^+}) \right]. \quad (\text{A7})$$

The loop integration factors are given by

$$I_1(m_1, m_2, m_3, m_4) = \int [dX] \frac{xy}{-x(1-x)m_1^2 + xz(m_1^2 - m_2^2) + (z+y)m_3^2 + xm_4^2}, \quad (\text{A8})$$

$$I_2(m_1, m_2, m_3, m_4) = \int [dX] \frac{xz}{-x(1-x)m_1^2 + xz(m_1^2 - m_2^2) + (z+y)m_3^2 + xm_4^2}, \quad (\text{A9})$$

$$I_3(m_1, m_2, m_3, m_4) = \int [dX] \frac{1-x}{-x(1-x)m_1^2 + xz(m_1^2 - m_2^2) + (z+y)m_3^2 + xm_4^2}, \quad (\text{A10})$$

$$I_4(m_1, m_2, m_3) = \int [dX] \frac{xy}{-x(1-x)m_1^2 + xz(m_1^2 - m_2^2) + (z+y)m_3^2}, \quad (\text{A11})$$

$$I_5(m_1, m_2, m_3) = \int [dX] \frac{xz}{-x(1-x)m_1^2 + xz(m_1^2 - m_2^2) + (z+y)m_3^2}, \quad (\text{A12})$$

where $\int [dX] \equiv \int_0^1 dx dy dz \delta(1-x-y-z)$.

Appendix B: List of viable models

In this appendix, we list viable models which can in principle fit neutrino data. The viable models under Z_4^{NI} , Z_5^{NI} , Z_6^{NI} and Z_7^{NI} are summarized in Table III, Table IV, Table V, and Tables VI-VIII, respectively.

[1] Y. Cai, J. Herrero-García, M. A. Schmidt, A. Vicente, and R. R. Volkas, *Front. in Phys.* **5**, 63 (2017), 1706.08524.

Z_4^{NI} Models	$\{k_{\ell 1}, k_{\ell 2}, k_{\ell 3}\}$	k_S	k_Φ	f	y^Φ	M_ℓ	m_ν	$m_\nu _{t_\beta \rightarrow \infty}$
(1)	$\{0, 1, 2\}$	1	1	$\begin{pmatrix} 0 & \times & 0 \\ \times & 0 & \times \\ 0 & \times & 0 \end{pmatrix}$	$\begin{pmatrix} 0 & \times & 0 \\ \times & 0 & \times \\ 0 & \times & 0 \end{pmatrix}$	$\begin{pmatrix} \times & \times & 0 \\ \times & \times & \times \\ 0 & \times & \times \end{pmatrix}$	$\begin{pmatrix} \times & \times & \times \\ \times & \times & \times \\ \times & \times & \times \end{pmatrix}$	$\begin{pmatrix} \times & 0 & \times \\ 0 & \times & 0 \\ \times & 0 & \times \end{pmatrix}$
(2)	$\{0, 1, 2\}$	2	1	$\begin{pmatrix} 0 & \times & 0 \\ \times & 0 & \times \\ 0 & \times & 0 \end{pmatrix}$	$\begin{pmatrix} 0 & 0 & \times \\ 0 & \times & 0 \\ \times & 0 & 0 \end{pmatrix}$	$\begin{pmatrix} \times & \times & 0 \\ \times & \times & \times \\ 0 & \times & \times \end{pmatrix}$	$\begin{pmatrix} \times & \times & \times \\ \times & 0 & \times \\ \times & \times & \times \end{pmatrix}$	$\begin{pmatrix} 0 & \times & 0 \\ \times & 0 & \times \\ 0 & \times & 0 \end{pmatrix}$

TABLE III: Viable assignments under Z_4^{NI} and structures of Yukawa and mass matrices. The structures obtained by exchanging and/or taking permutation among $\{k_{\ell 1}, k_{\ell 2}, k_{\ell 3}\}$ are also possible. It is the same for the tables afterwards.

Z_5^{NI} Models	$\{k_{\ell 1}, k_{\ell 2}, k_{\ell 3}\}$	k_S	k_Φ	f	y^Φ	M_ℓ	m_ν	$m_\nu _{t_\beta \rightarrow \infty}$
(1)	$\{0, 1, 2\}$	1	1	$\begin{pmatrix} 0 & \times & 0 \\ \times & 0 & \times \\ 0 & \times & 0 \end{pmatrix}$	$\begin{pmatrix} 0 & \times & 0 \\ \times & 0 & \times \\ 0 & \times & \times \end{pmatrix}$	$\begin{pmatrix} \times & \times & 0 \\ \times & \times & \times \\ 0 & \times & \times \end{pmatrix}$	$\begin{pmatrix} \times & \times & \times \\ \times & \times & \times \\ \times & \times & \times \end{pmatrix}$	$\begin{pmatrix} \times & 0 & \times \\ 0 & \times & \times \\ \times & \times & \times \end{pmatrix}$
(2)	$\{0, 1, 2\}$	1	2	$\begin{pmatrix} 0 & \times & 0 \\ \times & 0 & \times \\ 0 & \times & 0 \end{pmatrix}$	$\begin{pmatrix} 0 & 0 & \times \\ 0 & \times & \times \\ \times & \times & 0 \end{pmatrix}$	$\begin{pmatrix} \times & 0 & \times \\ 0 & \times & \times \\ \times & \times & \times \end{pmatrix}$	$\begin{pmatrix} \times & \times & \times \\ \times & \times & \times \\ \times & \times & \times \end{pmatrix}$	$\begin{pmatrix} 0 & \times & \times \\ \times & \times & \times \\ \times & \times & \times \end{pmatrix}$
(3)	$\{0, 1, 2\}$	2	1	$\begin{pmatrix} 0 & 0 & \times \\ 0 & 0 & \times \\ \times & \times & 0 \end{pmatrix}$	$\begin{pmatrix} 0 & \times & 0 \\ \times & 0 & \times \\ 0 & \times & \times \end{pmatrix}$	$\begin{pmatrix} \times & \times & 0 \\ \times & \times & \times \\ 0 & \times & \times \end{pmatrix}$	$\begin{pmatrix} \times & \times & \times \\ \times & \times & \times \\ \times & \times & \times \end{pmatrix}$	$\begin{pmatrix} 0 & \times & \times \\ \times & \times & \times \\ \times & \times & \times \end{pmatrix}$
(4)	$\{0, 1, 2\}$	2	2	$\begin{pmatrix} 0 & 0 & \times \\ 0 & 0 & \times \\ \times & \times & 0 \end{pmatrix}$	$\begin{pmatrix} 0 & 0 & \times \\ 0 & \times & \times \\ \times & \times & \times \end{pmatrix}$	$\begin{pmatrix} \times & \times & 0 \\ \times & \times & \times \\ 0 & \times & \times \end{pmatrix}$	$\begin{pmatrix} \times & \times & \times \\ \times & \times & \times \\ \times & \times & \times \end{pmatrix}$	$\begin{pmatrix} \times & \times & 0 \\ \times & \times & \times \\ 0 & \times & \times \end{pmatrix}$

TABLE IV: Viable assignments under Z_5^{NI} and structures of Yukawa and mass matrices.

- [2] A. Zee, Phys. Lett. **93B**, 389 (1980), [Erratum: Phys. Lett.95B,461(1980)].
- [3] J. Herrero-García, T. Ohlsson, S. Riad, and J. Wirén, JHEP **04**, 130 (2017), 1701.05345.
- [4] Y. Koide, Phys. Rev. D **64**, 077301 (2001), hep-ph/0104226.
- [5] P. H. Frampton, M. C. Oh, and T. Yoshikawa, Phys. Rev. D **65**, 073014 (2002), hep-

Z_6^{NI} Models	$\{k_{\ell 1}, k_{\ell 2}, k_{\ell 3}\}$	k_S	k_Φ	f	y^Φ	M_ℓ	m_ν	$m_\nu _{t_\beta \rightarrow \infty}$
(1)	$\{0, 1, 2\}$	1	1	$\begin{pmatrix} 0 & \times & 0 \\ \times & 0 & \times \\ 0 & \times & 0 \end{pmatrix}$	$\begin{pmatrix} 0 & \times & 0 \\ \times & 0 & \times \\ 0 & \times & 0 \end{pmatrix}$	$\begin{pmatrix} \times & \times & 0 \\ \times & \times & \times \\ 0 & \times & \times \end{pmatrix}$	$\begin{pmatrix} \times & \times & \times \\ \times & \times & \times \\ \times & \times & \times \end{pmatrix}$	$\begin{pmatrix} \times & 0 & \times \\ 0 & \times & 0 \\ \times & 0 & \times \end{pmatrix}$
(2)	$\{0, 1, 2\}$	1	3	$\begin{pmatrix} 0 & \times & 0 \\ \times & 0 & \times \\ 0 & \times & 0 \end{pmatrix}$	$\begin{pmatrix} 0 & 0 & 0 \\ 0 & 0 & \times \\ 0 & \times & 0 \end{pmatrix}$	$\begin{pmatrix} \times & 0 & 0 \\ 0 & \times & \times \\ 0 & \times & \times \end{pmatrix}$	$\begin{pmatrix} 0 & \times & \times \\ \times & \times & \times \\ \times & \times & \times \end{pmatrix}$	$\begin{pmatrix} 0 & 0 & \times \\ 0 & \times & 0 \\ \times & 0 & \times \end{pmatrix}$
(3)	$\{0, 1, 2\}$	2	1	$\begin{pmatrix} 0 & 0 & \times \\ 0 & 0 & 0 \\ \times & 0 & 0 \end{pmatrix}$	$\begin{pmatrix} 0 & \times & 0 \\ \times & 0 & \times \\ 0 & \times & 0 \end{pmatrix}$	$\begin{pmatrix} \times & \times & 0 \\ \times & \times & \times \\ 0 & \times & \times \end{pmatrix}$	$\begin{pmatrix} \times & \times & \times \\ \times & 0 & \times \\ \times & \times & \times \end{pmatrix}$	$\begin{pmatrix} 0 & \times & 0 \\ \times & 0 & \times \\ 0 & \times & 0 \end{pmatrix}$
(4)	$\{0, 1, 2\}$	3	1	$\begin{pmatrix} 0 & 0 & 0 \\ 0 & 0 & \times \\ 0 & \times & 0 \end{pmatrix}$	$\begin{pmatrix} 0 & \times & 0 \\ \times & 0 & \times \\ 0 & \times & 0 \end{pmatrix}$	$\begin{pmatrix} \times & \times & 0 \\ \times & \times & \times \\ 0 & \times & \times \end{pmatrix}$	$\begin{pmatrix} 0 & \times & \times \\ \times & \times & \times \\ \times & \times & \times \end{pmatrix}$	$\begin{pmatrix} 0 & 0 & \times \\ 0 & \times & 0 \\ \times & 0 & \times \end{pmatrix}$
(5)	$\{1, 2, 3\}$	1	1	$\begin{pmatrix} 0 & \times & 0 \\ \times & 0 & \times \\ 0 & \times & 0 \end{pmatrix}$	$\begin{pmatrix} 0 & \times & 0 \\ \times & 0 & \times \\ 0 & \times & 0 \end{pmatrix}$	$\begin{pmatrix} \times & \times & 0 \\ \times & \times & \times \\ 0 & \times & \times \end{pmatrix}$	$\begin{pmatrix} \times & \times & \times \\ \times & \times & \times \\ \times & \times & \times \end{pmatrix}$	$\begin{pmatrix} \times & 0 & \times \\ 0 & \times & 0 \\ \times & 0 & \times \end{pmatrix}$
(6)	$\{1, 2, 3\}$	1	3	$\begin{pmatrix} 0 & \times & 0 \\ \times & 0 & \times \\ 0 & \times & 0 \end{pmatrix}$	$\begin{pmatrix} 0 & \times & 0 \\ \times & 0 & 0 \\ 0 & 0 & 0 \end{pmatrix}$	$\begin{pmatrix} \times & \times & 0 \\ \times & \times & 0 \\ 0 & 0 & \times \end{pmatrix}$	$\begin{pmatrix} \times & \times & \times \\ \times & \times & \times \\ \times & \times & 0 \end{pmatrix}$	$\begin{pmatrix} \times & 0 & \times \\ 0 & \times & 0 \\ \times & 0 & 0 \end{pmatrix}$
(7)	$\{1, 2, 3\}$	2	1	$\begin{pmatrix} 0 & 0 & \times \\ 0 & 0 & 0 \\ \times & 0 & 0 \end{pmatrix}$	$\begin{pmatrix} 0 & \times & 0 \\ \times & 0 & \times \\ 0 & \times & 0 \end{pmatrix}$	$\begin{pmatrix} \times & \times & 0 \\ \times & \times & \times \\ 0 & \times & \times \end{pmatrix}$	$\begin{pmatrix} \times & \times & \times \\ \times & 0 & \times \\ \times & \times & \times \end{pmatrix}$	$\begin{pmatrix} 0 & \times & 0 \\ \times & 0 & \times \\ 0 & \times & 0 \end{pmatrix}$
(8)	$\{1, 2, 3\}$	3	1	$\begin{pmatrix} 0 & \times & 0 \\ \times & 0 & 0 \\ 0 & 0 & 0 \end{pmatrix}$	$\begin{pmatrix} 0 & \times & 0 \\ \times & 0 & \times \\ 0 & \times & 0 \end{pmatrix}$	$\begin{pmatrix} \times & \times & 0 \\ \times & \times & \times \\ 0 & \times & \times \end{pmatrix}$	$\begin{pmatrix} \times & \times & \times \\ \times & \times & \times \\ \times & \times & 0 \end{pmatrix}$	$\begin{pmatrix} \times & 0 & \times \\ 0 & \times & 0 \\ \times & 0 & 0 \end{pmatrix}$

TABLE V: Viable assignments under Z_6^{NI} and structures of Yukawa and mass matrices.

ph/0110300.

[6] X.-G. He, Eur. Phys. J. C **34**, 371 (2004), hep-ph/0307172.

[7] T. Fukuyama, H. Sugiyama, and K. Tsumura, Phys. Rev. D **83**, 056016 (2011), 1012.4886.

- [8] S. Kanemura, T. Shindou, and H. Sugiyama, *Phys. Rev. D* **92**, 115001 (2015), 1508.05616.
- [9] T. Nomura and K. Yagyu, *JHEP* **10**, 105 (2019), 1905.11568.
- [10] T. Matsui, T. Nomura, and K. Yagyu, *Nucl. Phys. B* **971**, 115523 (2021), 2102.09247.
- [11] F. Feruglio, *Are neutrino masses modular forms?* (2019), pp. 227–266, 1706.08749.
- [12] T. Nomura, H. Okada, and Y.-h. Qi, *Eur. Phys. J. C* **85**, 134 (2025), 2111.10944.
- [13] T. Nomura and H. Okada, *Phys. Lett. B* **867**, 139618 (2025), 2412.18095.
- [14] P. R. S. Gomes, *SciPost Phys. Lect. Notes* **74**, 1 (2023), 2303.01817.
- [15] S. Schafer-Nameki, *Phys. Rept.* **1063**, 1 (2024), 2305.18296.
- [16] L. Bhardwaj, L. E. Bottini, L. Fraser-Taliente, L. Gladden, D. S. W. Gould, A. Platschorre, and H. Tillim, *Phys. Rept.* **1051**, 1 (2024), 2307.07547.
- [17] S.-H. Shao (2023), 2308.00747.
- [18] T. Kobayashi and H. Otsuka, *JHEP* **11**, 120 (2024), 2408.13984.
- [19] T. Kobayashi, H. Otsuka, and M. Tanimoto, *JHEP* **12**, 117 (2024), 2409.05270.
- [20] A. Delgado and S. Koren, *JHEP* **02**, 178 (2025), 2412.05362.
- [21] S. Funakoshi, T. Kobayashi, and H. Otsuka, *JHEP* **04**, 183 (2025), 2412.12524.
- [22] T. Kobayashi, Y. Nishioka, H. Otsuka, and M. Tanimoto, *JHEP* **05**, 177 (2025), 2503.09966.
- [23] Q. Liang and T. T. Yanagida, *Phys. Lett. B* **868**, 139706 (2025), 2505.05142.
- [24] T. Kobayashi, H. Otsuka, M. Tanimoto, and H. Uchida (2025), 2505.07262.
- [25] T. Kobayashi, H. Okada, and H. Otsuka (2025), 2505.14878.
- [26] T. Kobayashi, H. Mita, H. Otsuka, and R. Sakuma (2025), 2506.10241.
- [27] T. Nomura and H. Okada (2025), 2506.16706.
- [28] J. Dong, T. Jeric, T. Kobayashi, R. Nishida, and H. Otsuka (2025), 2507.02375.
- [29] M. Suzuki and L.-X. Xu (2025), 2503.19964.
- [30] C. Cordova, S. Hong, S. Koren, and K. Ohmori, *Phys. Rev. X* **14**, 031033 (2024), 2211.07639.
- [31] T. Nomura and O. Popov (2025), 2507.10299.
- [32] J. Chen, C.-Q. Geng, H. Okada, and J.-J. Wu, *Nucl. Phys. B* **1025**, 117391 (2026), 2507.11951.
- [33] H. Okada and Y. Shigekami (2025), 2507.16198.
- [34] T. Kobayashi, H. Otsuka, and T. T. Yanagida, *Phys. Rev. D* **113**, 055016 (2026), 2508.12287.
- [35] M. Suzuki, L.-X. Xu, and H. Y. Zhang (2025), 2508.14970.
- [36] S. Jangid and H. Okada (2025), 2508.16174.
- [37] S. Jangid and H. Okada (2025), 2510.17292.

- [38] T. Nomura, H. Okada, and Y. Shigekami (2025), 2510.17156.
- [39] M. Suzuki and L.-X. Xu, JHEP **02**, 227 (2026), 2510.18972.
- [40] H. Okada and Y. Shoji (2025), 2512.20891.
- [41] Y. Nakai, H. Otsuka, Y. Shigekami, and Z. Zhang (2025), 2512.21509.
- [42] H. Okada and Y. Shigekami (2026), 2601.15749.
- [43] S. K. Kang, R. Kumar, and H. Okada (2026), 2601.22740.
- [44] M. Kashav (2026), 2602.14644.
- [45] H. Okada and J.-J. Wu (2026), 2603.17587.
- [46] H. Okada and H. Otsuka (2026), 2604.04423.
- [47] L.-X. Xu (2026), 2604.09345.
- [48] H. Okada and L. Singh (2026), 2604.11308.
- [49] T. Nomura and H. Okada (2026), 2604.27612.
- [50] J. J. Heckman, J. McNamara, M. Montero, A. Sharon, C. Vafa, and I. Valenzuela, Phys. Rev. D **110**, 106001 (2024), 2402.00118.
- [51] J. Kaidi, Y. Tachikawa, and H. Y. Zhang, SciPost Phys. **17**, 169 (2024), 2402.00105.
- [52] Y. Kuno and Y. Okada, Rev. Mod. Phys. **73**, 151 (2001), hep-ph/9909265.
- [53] R. Kitano, M. Koike, and Y. Okada, Phys. Rev. D **66**, 096002 (2002), [Erratum: Phys.Rev.D 76, 059902 (2007)], hep-ph/0203110.
- [54] S. Davidson, Y. Kuno, and M. Yamanaka, Phys. Lett. B **790**, 380 (2019), 1810.01884.
- [55] Y. G. Cui et al. (COMET) (2009).
- [56] K. Afanaciev et al. (MEG II), Eur. Phys. J. C **85**, 1177 (2025), [Erratum: Eur.Phys.J.C 85, 1317 (2025)], 2504.15711.
- [57] K. Afanaciev et al. (MEG II), Eur. Phys. J. C **84**, 216 (2024), [Erratum: Eur.Phys.J.C 84, 1042 (2024)], 2310.12614.
- [58] B. Aubert et al. (BaBar), Phys. Rev. Lett. **104**, 021802 (2010), 0908.2381.
- [59] A. Abdesselam et al. (Belle), JHEP **10**, 19 (2021), 2103.12994.
- [60] U. Bellgardt et al. (SINDRUM), Nucl. Phys. B **299**, 1 (1988).
- [61] K. Hayasaka et al., Phys. Lett. B **687**, 139 (2010), 1001.3221.
- [62] H. Okada and M. Tanimoto, Eur. Phys. J. C **81**, 52 (2021), 1905.13421.
- [63] S. Abe et al. (KamLAND-Zen) (2024), 2406.11438.
- [64] N. Abgrall et al. (LEGEND) (2021), 2107.11462.

- [65] G. Adhikari et al. (nEXO), *J. Phys. G* **49**, 015104 (2022), 2106.16243.
- [66] M. Aker et al. (KATRIN), *Science* **388**, adq9592 (2025), 2406.13516.
- [67] N. Aghanim et al. (Planck), *Astron. Astrophys.* **641**, A6 (2020), [Erratum: *Astron.Astrophys.* **652**, C4 (2021)], 1807.06209.
- [68] A. G. Adame et al. (DESI), *JCAP* **02**, 021 (2025), 2404.03002.
- [69] I. Esteban, M. C. Gonzalez-Garcia, M. Maltoni, I. Martinez-Soler, J. P. Pinheiro, and T. Schwetz, *JHEP* **12**, 216 (2024), 2410.05380.
- [70] K. Abazajian et al. (2019), 1907.04473.
- [71] T. Matsumura et al., *J. Low Temp. Phys.* **176**, 733 (2014), 1311.2847.
- [72] M. Sajjad Athar et al., *Prog. Part. Nucl. Phys.* **124**, 103947 (2022), 2111.07586.
- [73] A. Abada et al. (FCC), *Eur. Phys. J. C* **79**, 474 (2019).
- [74] M. Benedikt et al. (FCC), *Eur. Phys. J. C* **85**, 1468 (2025), 2505.00272.
- [75] W. Abdallah et al. (CEPC Study Group), *Radiat. Detect. Technol. Methods* **8**, 1 (2024), [Erratum: *Radiat.Detect.Technol.Methods* **9**, 184–192 (2025)], 2312.14363.
- [76] X. Ai et al., *Chin. Phys. C* **49**, 123108 (2025), 2505.24810.
- [77] S. P. Adhya et al. (CEPC Study Group) (2025), 2510.05260.
- [78] C. Accettura et al., *Eur. Phys. J. C* **83**, 864 (2023), [Erratum: *Eur.Phys.J.C* **84**, 36 (2024)], 2303.08533.
- [79] Y. Hamada, R. Kitano, R. Matsudo, H. Takaura, and M. Yoshida, *PTEP* **2022**, 053B02 (2022), 2201.06664.

Z_7^{NI} Models	$\{k_{\ell 1}, k_{\ell 2}, k_{\ell 3}\}$	k_S	k_Φ	f	y^Φ	M_ℓ	m_ν	$m_\nu _{t_\beta \rightarrow \infty}$
(10)	$\{0, 2, 3\}$	2	2	$\begin{pmatrix} 0 \times 0 \\ \times 0 \times \\ 0 \times 0 \end{pmatrix}$	$\begin{pmatrix} 0 \times 0 \\ \times 0 \times \\ 0 \times 0 \end{pmatrix}$	$\begin{pmatrix} \times \times 0 \\ \times \times \times \\ 0 \times \times \end{pmatrix}$	$\begin{pmatrix} \times \times \times \\ \times \times \times \\ \times \times \times \end{pmatrix}$	$\begin{pmatrix} \times 0 \times \\ 0 \times 0 \\ \times 0 \times \end{pmatrix}$
(11)	$\{0, 2, 3\}$	3	2	$\begin{pmatrix} 0 0 \times \\ 0 0 0 \\ \times 0 0 \end{pmatrix}$	$\begin{pmatrix} 0 \times 0 \\ \times 0 \times \\ 0 \times 0 \end{pmatrix}$	$\begin{pmatrix} \times \times 0 \\ \times \times \times \\ 0 \times \times \end{pmatrix}$	$\begin{pmatrix} \times \times \times \\ \times 0 \times \\ \times \times \times \end{pmatrix}$	$\begin{pmatrix} 0 \times 0 \\ \times 0 \times \\ 0 \times 0 \end{pmatrix}$
(12)	$\{1, 2, 3\}$	1	1	$\begin{pmatrix} 0 \times 0 \\ \times 0 \times \\ 0 \times 0 \end{pmatrix}$	$\begin{pmatrix} 0 \times 0 \\ \times 0 \times \\ 0 \times \times \end{pmatrix}$	$\begin{pmatrix} \times \times 0 \\ \times \times \times \\ 0 \times \times \end{pmatrix}$	$\begin{pmatrix} \times \times \times \\ \times \times \times \\ \times \times \times \end{pmatrix}$	$\begin{pmatrix} \times 0 \times \\ 0 \times \times \\ \times \times \times \end{pmatrix}$
(13)	$\{1, 2, 3\}$	1	2	$\begin{pmatrix} 0 \times 0 \\ \times 0 \times \\ 0 \times 0 \end{pmatrix}$	$\begin{pmatrix} \times 0 \times \\ 0 0 \times \\ \times \times \times \end{pmatrix}$	$\begin{pmatrix} \times 0 \times \\ 0 \times \times \\ \times \times \times \end{pmatrix}$	$\begin{pmatrix} \times \times \times \\ \times \times \times \\ \times \times \times \end{pmatrix}$	$\begin{pmatrix} 0 \times \times \\ \times \times \times \\ \times \times \times \end{pmatrix}$
(14)	$\{1, 2, 3\}$	1	3	$\begin{pmatrix} 0 \times 0 \\ \times 0 \times \\ 0 \times 0 \end{pmatrix}$	$\begin{pmatrix} 0 \times \times \\ \times \times 0 \\ \times 0 0 \end{pmatrix}$	$\begin{pmatrix} \times \times \times \\ \times \times 0 \\ \times 0 \times \end{pmatrix}$	$\begin{pmatrix} \times \times \times \\ \times \times \times \\ \times \times \times \end{pmatrix}$	$\begin{pmatrix} \times \times \times \\ \times \times \times \\ \times \times 0 \end{pmatrix}$
(15)	$\{1, 2, 3\}$	2	1	$\begin{pmatrix} 0 0 \times \\ 0 0 \times \\ \times \times 0 \end{pmatrix}$	$\begin{pmatrix} 0 \times 0 \\ \times 0 \times \\ 0 \times \times \end{pmatrix}$	$\begin{pmatrix} \times \times 0 \\ \times \times \times \\ 0 \times \times \end{pmatrix}$	$\begin{pmatrix} \times \times \times \\ \times \times \times \\ \times \times \times \end{pmatrix}$	$\begin{pmatrix} 0 \times \times \\ \times \times \times \\ \times \times \times \end{pmatrix}$
(16)	$\{1, 2, 3\}$	2	2	$\begin{pmatrix} 0 0 \times \\ 0 0 \times \\ \times \times 0 \end{pmatrix}$	$\begin{pmatrix} \times 0 \times \\ 0 0 \times \\ \times \times \times \end{pmatrix}$	$\begin{pmatrix} \times 0 \times \\ 0 \times \times \\ \times \times \times \end{pmatrix}$	$\begin{pmatrix} \times \times \times \\ \times \times \times \\ \times \times \times \end{pmatrix}$	$\begin{pmatrix} \times \times \times \\ \times \times 0 \\ \times 0 \times \end{pmatrix}$
(17)	$\{1, 2, 3\}$	2	3	$\begin{pmatrix} 0 0 \times \\ 0 0 \times \\ \times \times 0 \end{pmatrix}$	$\begin{pmatrix} 0 \times \times \\ \times \times 0 \\ \times 0 0 \end{pmatrix}$	$\begin{pmatrix} \times \times \times \\ \times \times 0 \\ \times 0 \times \end{pmatrix}$	$\begin{pmatrix} \times \times \times \\ \times \times \times \\ \times \times \times \end{pmatrix}$	$\begin{pmatrix} \times \times \times \\ \times 0 \times \\ \times \times \times \end{pmatrix}$
(18)	$\{1, 2, 3\}$	3	1	$\begin{pmatrix} 0 \times \times \\ \times 0 0 \\ \times 0 0 \end{pmatrix}$	$\begin{pmatrix} 0 \times 0 \\ \times 0 \times \\ 0 \times \times \end{pmatrix}$	$\begin{pmatrix} \times \times 0 \\ \times \times \times \\ 0 \times \times \end{pmatrix}$	$\begin{pmatrix} \times \times \times \\ \times \times \times \\ \times \times \times \end{pmatrix}$	$\begin{pmatrix} \times \times \times \\ \times \times \times \\ \times \times 0 \end{pmatrix}$

TABLE VII: Viable assignments under Z_7^{NI} and structures of Yukawa and mass matrices.

Z_7^{NI} Models	$\{k_{\ell 1}, k_{\ell 2}, k_{\ell 3}\}$	k_S	k_Φ	f	y^Φ	M_ℓ	m_ν	$m_\nu _{t_\beta \rightarrow \infty}$
(19)	$\{1, 2, 3\}$	3	2	$\begin{pmatrix} 0 & \times & \times \\ \times & 0 & 0 \\ \times & 0 & 0 \end{pmatrix}$	$\begin{pmatrix} \times & 0 & \times \\ 0 & 0 & \times \\ \times & \times & 0 \end{pmatrix}$	$\begin{pmatrix} \times & 0 & \times \\ 0 & \times & \times \\ \times & \times & \times \end{pmatrix}$	$\begin{pmatrix} \times & \times & \times \\ \times & \times & \times \\ \times & \times & \times \end{pmatrix}$	$\begin{pmatrix} \times & \times & \times \\ \times & 0 & \times \\ \times & \times & \times \end{pmatrix}$
(20)	$\{1, 2, 3\}$	3	3	$\begin{pmatrix} 0 & \times & \times \\ \times & 0 & 0 \\ \times & 0 & 0 \end{pmatrix}$	$\begin{pmatrix} 0 & \times & \times \\ \times & \times & 0 \\ \times & 0 & 0 \end{pmatrix}$	$\begin{pmatrix} \times & \times & \times \\ \times & \times & 0 \\ \times & 0 & \times \end{pmatrix}$	$\begin{pmatrix} \times & \times & \times \\ \times & \times & \times \\ \times & \times & \times \end{pmatrix}$	$\begin{pmatrix} \times & \times & 0 \\ \times & \times & \times \\ 0 & \times & \times \end{pmatrix}$

TABLE VIII: Viable assignments under Z_7^{NI} and structures of Yukawa and mass matrices.